

Search for Three-Nucleon Force Effects in Two-Body Photodisintegration of ${}^3\text{He}$ (${}^3\text{H}$) and in the Time Reversed Proton-Deuteron Radiative Capture Process

R. Skibiński¹, J. Golak^{1,2}, H. Kamada³ H. Witała¹, W. Glöckle², A. Nogga⁴.

¹*M. Smoluchowski Institute of Physics, Jagiellonian University, PL-30059 Kraków, Poland*

²*Institut für Theoretische Physik II, Ruhr Universität Bochum, D-44780 Bochum, Germany*

³*Department of Physics, Faculty of Engineering, Kyushu Institute of Technology, 1-1 Sensuicho, Tobata, Kitakyushu 804-8550, Japan*

⁴*Department of Physics, University of Arizona, Tucson, Arizona 85721, USA*

(May 2, 2019)

Abstract

Faddeev calculations have been performed for nucleon-deuteron photodisintegration of ${}^3\text{He}$ (${}^3\text{H}$) and proton-deuteron radiative capture. The bulk of the results is based on the AV18 nucleon-nucleon force and the Urbana IX three-nucleon force together with explicit exchange currents or applying the Siegert approach. Three-nucleon force effects are predicted for both processes and supported by most of the data.

21.45.+v, 24.70.+s, 25.10.+s, 25.40.Lw

I. INTRODUCTION

Three-nucleon (3N) forces come more and more into the focus of few-nucleon studies. Pure 3N continuum measurements at the accelerator facilities IUCF [1], KVI [2], RIKEN [3] and RCNP [4] are performed around 100-200 MeV nucleon laboratory energies with the aim to confront data to theoretical predictions based on modern high-precision nucleon-nucleon (NN) forces only [5]. Clear-cut discrepancies for certain 3N observables against all those predictions can be considered to be good candidates for 3N force (3NF) effects. Thereby the theoretical investigations are based on numerically precise solutions of the 3N Faddeev equations. Then adding present day 3NF models and comparing to those data one tries to explore their strength and spin structure [6]. Right now these 3NF models are the 2π -exchange Tucson Melbourne (TM) [7], a modified version thereof, TM' [8], which is closer to chiral symmetry, and the Urbana IX [9] forces. Another path to learn about 3NF's is the study of the low lying spectra of light nuclei as performed in Greens function Monte Carlo calculations [10]. The inclusion of 3π -exchange ring diagrams with intermediate Δ 's on top of the Urbana IX 3NF appears to be rather promising to improve the theoretical description of the spectra [11].

Electromagnetically induced reactions in the 3N system should also show effects of 3NF's. It is the aim of this paper to investigate the nucleon-deuteron (Nd) photodisintegration of ^3He and ^3H as well as the time reversed proton-deuteron (pd) capture process using modern NN forces and various 3NF models.

The single nucleon current operator is supplemented by exchange currents either in the form of the Siegert approximation or by explicitly including MEC's of the π - and ρ -like nature. The treatment is carried through nonrelativistically, though presumably some of the data that we analyze, require at least relativistic corrections.

Two-body photodisintegration of ^3He (^3H) has a long history. Barbour and Phillips [12] found that the incorporation of the interacting 3N continuum is crucial for the understanding of that process. They solved the 3N Faddeev equations, at that time of course based on simple finite rank forces. This was taken up again more consistently by Gibson and Lehman [13] treating the 3N bound state and the final 3N continuum on equal footing. More recently the Bonn group [14,15] used more modern NN forces represented in finite rank form. They analyzed quite a few data and pointed out a correlation of a certain cross section peak height with the triton binding energy, an issue which we shall also address but now in the context of 3NF effects. All the work mentioned relied on the Siegert approximation. The current was restricted to the dominant E_1 multipole [14] or to the E_1 and E_2 multipoles [15]. In a recent paper [16] a benchmark was set on the total 3N photodisintegration cross section.

Also for the pd capture process many experimental and theoretical studies have been performed in the past. We refer to [15,17,18] for references. Specifically we want to point to the theoretical investigations by Schadow *et al.* [15], Fonseca and Lehman [19] and to recent studies at very low energies by Viviani *et al.* [20].

The present investigation is restricted to nucleon- deuteron fragmentations in relation to ^3He (^3H) and we refer to a forthcoming study for 3N fragmentations.

The paper is organized as follows. In Sec. II we briefly review our formalism and the dynamical ingredients. Our results for Nd photodisintegration are presented in Sec. III together with available data. The pd capture observables are discussed in Sec. IV. We

summarize in Sec. V.

II. FORMALISM

We evaluated photodisintegration and pd capture before in [18] and [21,22], always using Faddeev-like integral equations. In [22] we formulated pd capture based on NN forces alone. There the Faddeev-like integral equation is identical to the one for Nd scattering. This is because in pd capture the 3N scattering state $|\Psi^{(+)}\rangle$ enters directly. On the other hand in ${}^3\text{He}$ photodisintegration the 3N scattering state $\langle\Psi^{(-)}|$ is involved like in electrodisintegration of ${}^3\text{He}$. The way to derive Faddeev-like integral equations in the latter cases is to apply the adjoint Moeller wave operator entering the nuclear matrix element to the right, namely onto the electromagnetic current operator and the ${}^3\text{He}$ bound state [23]. This has the very big advantage that the driving term of that Faddeev-type integral equation is fully connected, namely proportional to the ${}^3\text{He}$ bound state. Because of the formal identity of the nuclear matrix elements for photodisintegration and electron induced processes the same Faddeev-like integral equation is applicable. In the two cases only the components of the current operator in the driving term have to be chosen appropriately. Now using time reversal symmetry one can relate the matrix elements for pd capture and photodisintegration, which are evaluated quite differently. This is a highly nontrivial numerical test for the various complex numerical steps involved.

In [18] we added a 3NF in the evaluation of the pd capture process and applied it to cross sections and several spin observables. The formalism was straightforward since we could use directly the Faddeev-like integral equation for Nd scattering including 3N forces as derived in [24]. In the same paper [18] we compared Siegert approximation to the explicit use of a restricted but possibly dominant set of mesonic exchange currents.

Now for two- and three-body photodisintegration we would also like to formulate an extension including 3N forces. We shall proceed as follows. The nuclear matrix element for Nd-photodisintegration of a 3N bound state has the following form

$$N_{\tau}^{\text{Nd}} \equiv \langle\Psi_{\vec{q}}^{(-)}|j_{\tau}(\vec{Q})|\Psi_{\text{bound}}\rangle, \quad (1)$$

where \vec{q} is the asymptotic relative momentum between the proton and the deuteron, and $j_{\tau}(\vec{Q})$ is the component of the 3N current operator. The scattering state $\langle\Psi_{\vec{q}}^{(-)}|$ can be Faddeev decomposed

$$\langle\Psi_{\vec{q}}^{(-)}| = \langle\psi_{\vec{q}}^{(-)}|(1+P), \quad (2)$$

where P , according to our standard notation [25], is the sum of a cyclical and anticyclical permutation. The Faddeev amplitude $\langle\psi_{\vec{q}}^{(-)}|$ obeys the Faddeev equation [24]

$$\langle\psi_{\vec{q}}^{(-)}| = \langle\phi_{\vec{q}}| + \langle\psi_{\vec{q}}^{(-)}| \left(PtG_0 + (1+P)V_4^{(1)}G_0(tG_0+1) \right). \quad (3)$$

Here the channel state $\langle\phi_{\vec{q}}|$ enters, which is a product of a deuteron wave function and a momentum eigenstate of the remaining nucleon, the NN t-operator t acting on nucleons 2 and 3, the free 3N propagator G_0 , the permutation operator P and $V_4^{(1)}$, the part of a 3N force, which singles out particle 1. For our notation see [25] and [5].

Using Eqs. (1), (2) and (3) we can write the nuclear matrix element as

$$N_\tau^{\text{Nd}} = \langle \phi_{\vec{q}} | (1 - K)^{-1}(1 + P)j_\tau(\vec{Q}) | \Psi_{\text{bound}} \rangle, \quad (4)$$

where K is the kernel of the integral equation (3). We introduce

$$| U \rangle \equiv (1 - K)^{-1}(1 + P)j_\tau(\vec{Q}) | \Psi_{\text{bound}} \rangle \quad (5)$$

or explicitly the integral equation

$$| U \rangle = (1 + P)j_\tau(\vec{Q}) | \Psi_{\text{bound}} \rangle + \left(PtG_0 + (1 + P)V_4^{(1)}G_0(tG_0 + 1) \right) | U \rangle. \quad (6)$$

This form is not yet suitable for numerical applications because of the presence of P to the very left. This has already been noted at the very beginning of our numerical 3N studies using nuclear forces without finite rank representations [26]. To rewrite Eq. (6) into a suitable form we use the following obvious identities

$$(1 + P) = \frac{1}{2}P(1 + P) \quad (7)$$

$$\frac{1}{2}P(P - 1) = 1 \quad (8)$$

and obtain

$$\begin{aligned} (P - 1) | U \rangle &= (P - 1)(1 + P)j_\tau(\vec{Q}) | \Psi_{\text{bound}} \rangle + \\ &(P - 1)P \left(tG_0 + \frac{1}{2}(1 + P)V_4^{(1)}G_0(tG_0 + 1) \right) \frac{1}{2}P(P - 1) | U \rangle. \end{aligned} \quad (9)$$

This Faddeev-like integral equation is suitable for numerical implementations and has the form

$$\begin{aligned} | \tilde{U} \rangle &= (1 + P)j_\tau(\vec{Q}) | \Psi_{\text{bound}} \rangle + \\ &\left(tG_0P + \frac{1}{2}(1 + P)V_4^{(1)}G_0(tG_0 + 1)P \right) | \tilde{U} \rangle \end{aligned} \quad (10)$$

with

$$| \tilde{U} \rangle \equiv (P - 1) | U \rangle. \quad (11)$$

Then the nuclear matrix element results as

$$N_\tau^{\text{Nd}} = \frac{1}{2} \langle \phi_{\vec{q}} | P | \tilde{U} \rangle. \quad (12)$$

In view of a forthcoming paper we also describe now the treatment of the complete 3N break-up process. The nuclear matrix element is

$$N_\tau^{\text{3N}} \equiv \langle \Psi_{\vec{p}\vec{q}}^{(-)} | j_\tau(\vec{Q}) | \Psi_{\text{bound}} \rangle. \quad (13)$$

The asymptotic momenta of the three nucleons are given by standard Jacobi momenta \vec{p} and \vec{q} [25]. The Faddeev amplitude corresponding to the scattering state in Eq. (13) is now defined via

$$\langle \psi_{\vec{p}\vec{q}}^{(-)} | = {}^{(-)}\langle \vec{p}\vec{q} | + \langle \psi_{\vec{p}\vec{q}}^{(-)} | K, \quad (14)$$

where K is the same kernel as used before in Eq. (3) and

$${}^{(-)}\langle \vec{p}\vec{q} | \equiv \langle \phi_0 | (tG_0 + 1). \quad (15)$$

It is to be noted that the free two-body subsystem state in $\langle \phi_0 |$ is properly antisymmetrized. Here $\langle \phi_0 |$ is the free 3N state. Following the same steps as above one ends up with

$$N_{\tau}^{3N} = \frac{1}{2} \langle \phi_0 | (tG_0 + 1)P | \tilde{U} \rangle, \quad (16)$$

where $| \tilde{U} \rangle$ is as given above.

In the actual numerical calculation we used, however, another form, which for the purpose of completeness, we would also like to present here. The reason for that is that at the time of the installation, the very heavy numerical tasks were more easily performed with already existing building blocks. That alternative forms are for the Nd-break up

$$N_{\tau}^{Nd} = \langle \phi_{\vec{q}} | (1 + P) | j_{\tau}(\vec{Q}) | \Psi_{\text{bound}} \rangle + \langle \phi_{\vec{q}} | P | U' \rangle \quad (17)$$

and for the 3N break up

$$N_{\tau}^{3N} = \langle \phi_0 | (1 + P)j_{\tau}(\vec{Q}) | \Psi_{\text{bound}} \rangle + \langle \phi_0 | tG_0(1 + P)j_{\tau}(\vec{Q}) | \Psi_{\text{bound}} \rangle + \langle \phi_0 | P | U' \rangle + \langle \phi_0 | tG_0P | U' \rangle. \quad (18)$$

The Faddeev-like integral equation for $| U' \rangle$ reads then

$$| U' \rangle = \left(tG_0 + \frac{1}{2}(1 + P)V_4^{(1)}G_0(tG_0 + 1) \right) (1 + P)j_{\tau}(\vec{Q}) | \Psi_{\text{bound}} \rangle + \left(tG_0P + \frac{1}{2}(1 + P)V_4^{(1)}G_0(tG_0 + 1)P \right) | U' \rangle. \quad (19)$$

The equivalence between the matrix elements (12) and (16) on the one hand and (17) and (18) on the other hand is demonstrated as follows. From Eqs. (10) and (19) we have

$$\begin{aligned} & | \tilde{U} \rangle - | U' \rangle = \\ & (1 - K)^{-1} \left((1 + P)j_{\tau}(\vec{Q}) | \Psi_{\text{bound}} \rangle - tG_0(1 + P)j_{\tau}(\vec{Q}) | \Psi_{\text{bound}} \rangle - \right. \\ & \left. \frac{1}{2}(1 + P)V_4^{(1)}G_0(tG_0 + 1)(1 + P)j_{\tau}(\vec{Q}) | \Psi_{\text{bound}} \rangle \right) = \\ & (1 - K)^{-1} \left(1 - tG_0 - \frac{1}{2}(1 + P)V_4^{(1)}G_0(tG_0 + 1) \right) (1 + P)j_{\tau}(\vec{Q}) | \Psi_{\text{bound}} \rangle. \end{aligned} \quad (20)$$

Using again Eq. (7) and the form of the kernel K this is

$$| \tilde{U} \rangle - | U' \rangle =$$

$$\begin{aligned}
& (1 - K)^{-1} \frac{1}{2} (P - 1 + 1 - K) (1 + P) j_\tau(\vec{Q}) \mid \Psi_{\text{bound}} \rangle = \\
& \frac{1}{2} (1 - K)^{-1} (P - 1) (1 + P) j_\tau(\vec{Q}) \mid \Psi_{\text{bound}} \rangle + \frac{1}{2} (1 + P) j_\tau(\vec{Q}) \mid \Psi_{\text{bound}} \rangle = \\
& \frac{1}{2} (1 - K)^{-1} (1 + P) j_\tau(\vec{Q}) \mid \Psi_{\text{bound}} \rangle + \frac{1}{2} (1 + P) j_\tau(\vec{Q}) \mid \Psi_{\text{bound}} \rangle \equiv \\
& \frac{1}{2} \mid \tilde{U} \rangle + \frac{1}{2} (1 + P) j_\tau(\vec{Q}) \mid \Psi_{\text{bound}} \rangle. \tag{21}
\end{aligned}$$

Thus

$$\frac{1}{2} \mid \tilde{U} \rangle - \mid U' \rangle = \frac{1}{2} (1 + P) j_\tau(\vec{Q}) \mid \Psi_{\text{bound}} \rangle. \tag{22}$$

Now it is a simple task to verify that the two expressions for the 3N break-up amplitude (16) and (18) are identical. This is also true for the two Nd break-up amplitudes (12) and (17). It is efficient to evaluate also the pd capture process using time reversal in terms of the formalism just described. This is what we do in this paper.

III. RESULTS FOR PD (ND) PHOTODISINTEGRATION OF ${}^3\text{He}$ (${}^3\text{H}$).

We use the AV18 NN force [27] combined with the Urbana IX 3N force [9]. By construction that force combination describes the ${}^3\text{H}$ binding energy correctly. It overbinds however slightly the ${}^3\text{He}$ bound state energy by 21 keV [28]. Our calculations are fully converged by choosing total two- nucleon angular momenta up to $j_{\text{max}}=3$ and total 3N angular momenta up to $J_{\text{max}}=15/2$. It turned out to be sufficient to keep the 3N force different from zero for total 3N angular momenta up to $J=7/2$. The standard nonrelativistic form of the single nucleon current operator [29] is supplemented by exchange currents via the Siegert approximation. We use it in the form as detailed in [18]. In our treatment electric and magnetic multipoles are kept to a very high order (6–7) and no long wave length approximation is used. The formalism is performed throughout in momentum space.

We show in Fig. 1 the angular distribution for pd photodisintegration of ${}^3\text{He}$ against the angle between the outgoing deuteron and the incoming photon direction in the laboratory system. The photon energies E_γ vary between 10 and 140 MeV. At the two lower energies the cross section maximum is decreased by adding the 3NF. A related effect has been seen before in [14] using different NN forces. Thereby it was found, that with increasing binding energy the value of the maximum decreased. This can be considered as a scaling behavior with the 3N binding energy. It ceases to be valid for the higher energies, where the results including the 3N force overtake the ones without. At about $E_\gamma=28$ MeV the 3N force effects for the process ${}^3\text{He}(\gamma, d)p$ in that observable vanish.

Have these effects already been seen in some data? We are aware of cross section data at the deuteron laboratory and c.m. angles of 90° as a function of E_γ [31,30]. They are shown in Fig. 2 in comparison to our theoretical results. We see the crossing of the theoretical curves without and with 3NF's around 25 MeV and indeed the data support the decrease of the cross section at lower energy values as predicted by including the 3NF. At higher energies the effects of the 3NF appear to be somewhat too strong in case of the Ticcioli *et al.* data [30].

For $E_\gamma = 120$ MeV and higher photon energies we are aware of another set of data for that process [32,33]. The deuteron laboratory angle is 103° now. In this case the addition of the 3NF is clearly supported by the data and the agreement is very good. This is shown in Fig. 3.

There are also total nd and pd cross section data for the processes ${}^3\text{H}(\gamma, d)n$ and ${}^3\text{He}(\gamma, d)p$. We show them in Figs. 4 and 5. Clearly the old data for the nd cross section have too big error bars to be conclusive. In the case of the pd cross section the inclusion of the 3NF's deteriorates the agreement for the low photon energies. The nd cross section data have been displayed before in [16].

Summarizing, the comparison with the data appears to be somewhat contradictory since the decrease and increase of the cross sections due to 3NF effects at low and high energies are not always supported by the data.

In order to provide information on the dependence of the cross sections on the choice of forces and currents we display in Table I results for the total two-body photodisintegration cross section of ${}^3\text{He}$ (${}^3\text{H}$) at three energies. At 12 MeV we see 5 % (10 %) spreads with (without) 3NF's. At the higher energies the spreads are negligible. For all energies 3NF effects are nevertheless clearly visible.

IV. PD CAPTURE CROSS SECTIONS

In Ref. [18] cross sections and spin observables for pd capture have been investigated at proton laboratory energies E_p between 5 and 200 MeV (corresponding to deuteron laboratory energies E_d between 10 and 400 MeV). The emphasis was on testing the sensitivity of pd capture observables to changes in the choice of NN forces and to compare the predictions of the Siegert approximation to the ones including explicitly π - and ρ -like MEC's. We found that at low energies Siegert and MEC predictions are rather close together, whereas at the higher energies differences showed up. In the context of the Siegert approach the predictions based on different NN forces turned out to be rather close together, which is a satisfactory result, since it demonstrates stability. The agreement with the data was mostly good, but also clear discrepancies were present, which call for an improvement of the dynamical input. It is the aim of this paper to include 3NF's, which in the previous work were only marginally investigated.

In the following we show our results for cross sections between $E_d = 19.8$ MeV and $E_d = 400$ MeV. In all of the following figures four theoretical curves are displayed. They are based on the Siegert approach, the single nucleon current together with explicit π - and ρ -like MEC's consistent to the NN force, the Siegert with 3NF and MEC's with 3NF. Let us denote these four choices by a, b, a' and b', for short.

We see in Fig. 6 the pd capture cross section at $E_d = 19.8$ MeV. In both cases, Siegert and explicit MEC's, the inclusion of the 3NF decreases the cross section; in case of Siegert the decrease is much stronger. The choices a, b and b' are well within the error bars and only a' is significantly too low. At $E_d = 95$ MeV the cross section data are fairly well described by all four choices. This is displayed in Fig. 7. As already seen in the Nd photodisintegration the theoretical cross section increases by including 3NF's. This is in agreement with our findings for pd capture [18].

Finally we show the cross sections for $E_p = 100, 150$ and 200 MeV (corresponding to $E_d = 200, 300$ and 400 MeV) in Fig. 8. The cases with the explicit MEC's b and b' describe the data best. The choice a clearly underpredicts the maxima and a' overpredicts the tails at large angles.

Summarizing, there is room for improvements; the dynamics occurring in MEC's and 3NF's is not well enough understood.

V. SUMMARY AND CONCLUSIONS

We presented the formalisms for including 3NF's into the Faddeev framework for photodisintegration of three nucleon bound states. The resulting equations are solved rigorously using high precision nuclear forces: AV18 together with the Urbana IX 3NF or CD Bonn with TM 3NF. Many-body currents are included either in the form of π - and ρ -like exchanges related to AV18 or via the Siegert approach. The calculations are nonrelativistic but employ state of the art dynamics. We posed several questions. How well do the Siegert approach and the explicit use of the π - and ρ -like MEC's compare with each other? Our results show differences between the two approaches. This can be expected since not to all parts of the NN force corresponding MEC's have been taken into account to guarantee that the continuity equation is fulfilled with respect to the complete AV18 NN force. On the other hand the two results (Siegert and explicit MEC's) are also not too distinct from each other.

Another even more central question in that paper was to shed light on possible 3NF effects. In case of pd photodisintegration of ${}^3\text{He}$ we compared theoretical predictions without and with a 3NF. Here the old data generally support the predicted 3NF effects. For one case, however, the 3NF used did not improve the description of the data [37]. Renewed measurements should clarify the experimental situation.

For the cross section in pd capture at the higher energies, $E_p = 100$ MeV and above, the inclusion of the 3NF in the Siegert approach improves the agreement in the maximum but deteriorates it at the large backward angles, whereas the explicit use of MEC's together with 3NF's describes the data better.

Altogether the shifts caused by the Urbana IX 3NF on top of the AV18 NN force and explicit MEC's is supported by most of the data we analyzed. The Siegert approach is less successful. The use of other force combinations as exemplified in the total two-body photodisintegration cross section does not lead to alarming variations. High quality data would be very helpful to challenge theory more strongly.

ACKNOWLEDGMENTS

This work was supported by the Deutsche Forschungsgemeinschaft (H.K., A.N. and J.G.), the Polish Committee for Scientific Research under Grants No. 2P03B02818 and 2P03B05622 and by the NSF under Grant # PHY0070858. W.G. would like to thank the Foundation for Polish Science for the financial support during his stay in Cracow. R.S. is a holder of scholarship from the Foundation for Polish Science and acknowledges its financial support. The numerical calculations have been performed on the Cray T90 and T3E of the NIC in Jülich, Germany.

REFERENCES

- [1] H.O. Meyer, Mesons and Light Nuclei, 8th Conference, Prague, Czech Republic, July 2001, edited by J. Adam, P. Bydžovský and J. Mareš, AIP Conf. Proc. **603**, 113 (2001).
- [2] R. Bieber *et al.*, Phys. Rev. Lett. **84**, 606 (2000), K. Ermisch *et al.*, Phys. Rev. Lett. **86**, 5862 (2001) and N. Kalantar-Nayestanaki, private communication.
- [3] H. Sakai *et al.*, Few Body Syst. **Suppl. 12**, 403 (2000).
- [4] K. Sagara, ECT* Workshop, July 2001, Trento and private communication.
- [5] W. Glöckle, H. Witała, D. Hüber, H. Kamada and J. Golak, Phys. Rep. **274**, 107 (1996).
- [6] H. Witała *et al.*, Phys. Rev. **C63**, 024007 (2001).
- [7] S. A. Coon *et al.*, Nucl. Phys. **A318**, 242 (1979); S. A. Coon, W. Glöckle, Phys. Rev. C **23**, 1790 (1981).
- [8] J. L. Friar, D. Hüber, U. van Kolck, Phys. Rev. **C59**, 53 (1999).
- [9] B. S. Pudliner, V. R. Pandharipande, J. Carlson, Steven C. Pieper, and R. B. Wiringa, Phys. Rev. **C56**, 1720 (1997).
- [10] R. B. Wiringa, Steven C. Pieper, J. Carlson, V. R. Pandharipande, Phys. Rev. **C62**, 014001 (2000).
- [11] S.C. Pieper, V.R. Pandharipande, R.B. Wiringa, J. Carlson, Phys. Rev. **C64**, 014001 (2001).
- [12] I.M. Barbour, A.C. Phillips, Phys. Rev. **C1**, 165 (1970).
- [13] B.F. Gibson, D.R. Lehman, Phys. Rev. **C11**, 29 (1975).
- [14] W. Sandhas, W. Schadow, G. Ellerkmann, L.L. Howell, S.A. Sofianos, Nucl. Phys. **A631**, 210c (1998);
- [15] W. Schadow, O. Nohadani, W. Sandhas, Phys. Rev. **C63**, 044006 (2001).
- [16] J. Golak, R. Skibiński, W. Glöckle, H. Kamada, A. Nogga, H. Witała, V.D. Efros, W. Leidemann, G. Orlandini, and E.L. Tomusiak, nucl-th/0202014.
- [17] D. J. Klepaki, Y.E. Kim and R.A. Brandenburg, Nucl. Phys. **A 550**, 53 (1992).
- [18] J. Golak *et al.*, Phys. Rev. **C62**, 054005 (2000).
- [19] A. C. Fonseca and D. R. Lehman, Few-Body Syst. **28**, 189 (2000).
- [20] M. Viviani *et al.*, Phys. Rev. **C61**, 064001 (2000).
- [21] H. Kamada *et al.*, Nucl. Phys. **A 684**, 618c (2001).
- [22] H. Anklin, L.J. de Bever, S. Buttazzoni, W. Glöckle, J. Golak, A. Honegger, J. Jourdan, H. Kamada, G. Kubon, T. Petitjean, L.M. Qin, I. Sick, Ph. Steiner, H. Witała, M. Zeier, J. Zhao and B. Zihlmann, Nucl. Phys. **A636**, 189 (1998).
- [23] J. Golak *et al.*, Phys. Rev. **C51**, 1638 (1995).
- [24] D. Hüber, H. Kamada, H. Witała, and W. Glöckle, Acta Physica Polonica **B28**, 1677 (1997).
- [25] W. Glöckle, *The Quantum Mechanical Few-Body Problem*, Springer-Verlag, Berlin, 1983.
- [26] A. Bömelburg, W. Glöckle, W. Meier in Few Body Problems in Physics, vol. II, Contributed papers, B. Zeitnitz ed. (Elsevier Science Publishers: B.V. Amsterdam, 1984), p. 483.
- [27] R. B. Wiringa, V.G.J. Stoks, and R. Schiavilla, Phys. Rev. **C51**, 38 (1995).
- [28] A. Nogga, A. Kievsky, H. Kamada, W. Glöckle, L.E. Marcucci, S. Rosati, M. Viviani, nucl-th/0202037.
- [29] S. Ishikawa, K. Kamada, W. Glöckle, J. Golak, H. Witała, Il Nuovo Cimento, **107A**, 305 (1994).

- [30] G. Ticcioni, S.N. Gardiner, J.L. Matthews, and R.O. Owens, Phys. Lett. **46B**, 369 (1973).
- [31] J.R. Stewart, R. Morrison and J. O'Connell, Phys. Rev. **138**, B372 (1965).
- [32] D.I. Sober *et al.*, Phys. Rev. **C28**, 2234 (1983).
- [33] N.M. O'Fallon, L.Koester Jr. and J.Smith, Phys. Rev. **C5**, 1926 (1972).
- [34] D.D. Faul, B.L. Berman, P. Meyer and D.L. Olson, Phys. Rev. **C24**, 849 (1981).
- [35] D.M. Skopik *et al.*, Phys. Rev. **C24**, 1791 (1981).
- [36] R. Kosiek *et al.*, Phys. Lett. **21**, 199 (1966).
- [37] S.K. Kundu, Y.M. Shin and G.D. Wait, Nucl. Phys. **A171**, 384 (1971).
- [38] B. D. Belt, C. R. Bingham, M. L. Halbert, and A. van der Woude, Phys. Rev. Lett. **24**, 1120 (1970).
- [39] W. K. Pitts, H. O. Meyer, L. C. Bland, J. D. Brown, R. C. Byrd, M. Hugi, H. J. Karwowski, P. Schwandt, A. Sinha, J. Sowinski, I. J. van Heerden, A. Arriaga, F.D. Santos, Phys. Rev. **C37**, 1 (1988).
- [40] M. A. Pickar, H. J. Karwowski, J. D. Brown, J. R. Hall, M. Hugi, R. E. Pollock, V. R. Cupps, M. Fatyga, and A. D. Bacher, Phys. Rev. **C35**, 37 (1987).

TABLES

	$E_\gamma = 12$ [MeV]	$E_\gamma = 40$ [MeV]	$E_\gamma = 120$ [MeV]
AV18-Siegert	0.987 (1.014)	0.165 (0.166)	0.017 (0.015)
AV18-MEC	0.951 (0.947)	0.162 (0.155)	0.018 (0.015)
CD Bonn-Siegert	0.934 (0.930)	0.165 (0.169)	0.018 (0.016)
AV18+UrbanaIX-Siegert	0.845 (0.851)	0.177 (0.179)	0.022 (0.020)
AV18+UrbanaIX-MEC	0.916 (0.902)	0.174 (0.167)	0.021 (0.018)
CD Bonn+TM-Siegert	0.855 (0.831)	0.171 (0.175)	0.021 (0.020)
CD Bonn2000+TM'-Siegert	0.820 (0.844)	0.177 (0.177)	0.022 (0.019)

TABLE I. The total cross section (in mb) for two-body photodisintegration of ${}^3\text{He}$ (${}^3\text{H}$).

FIGURES

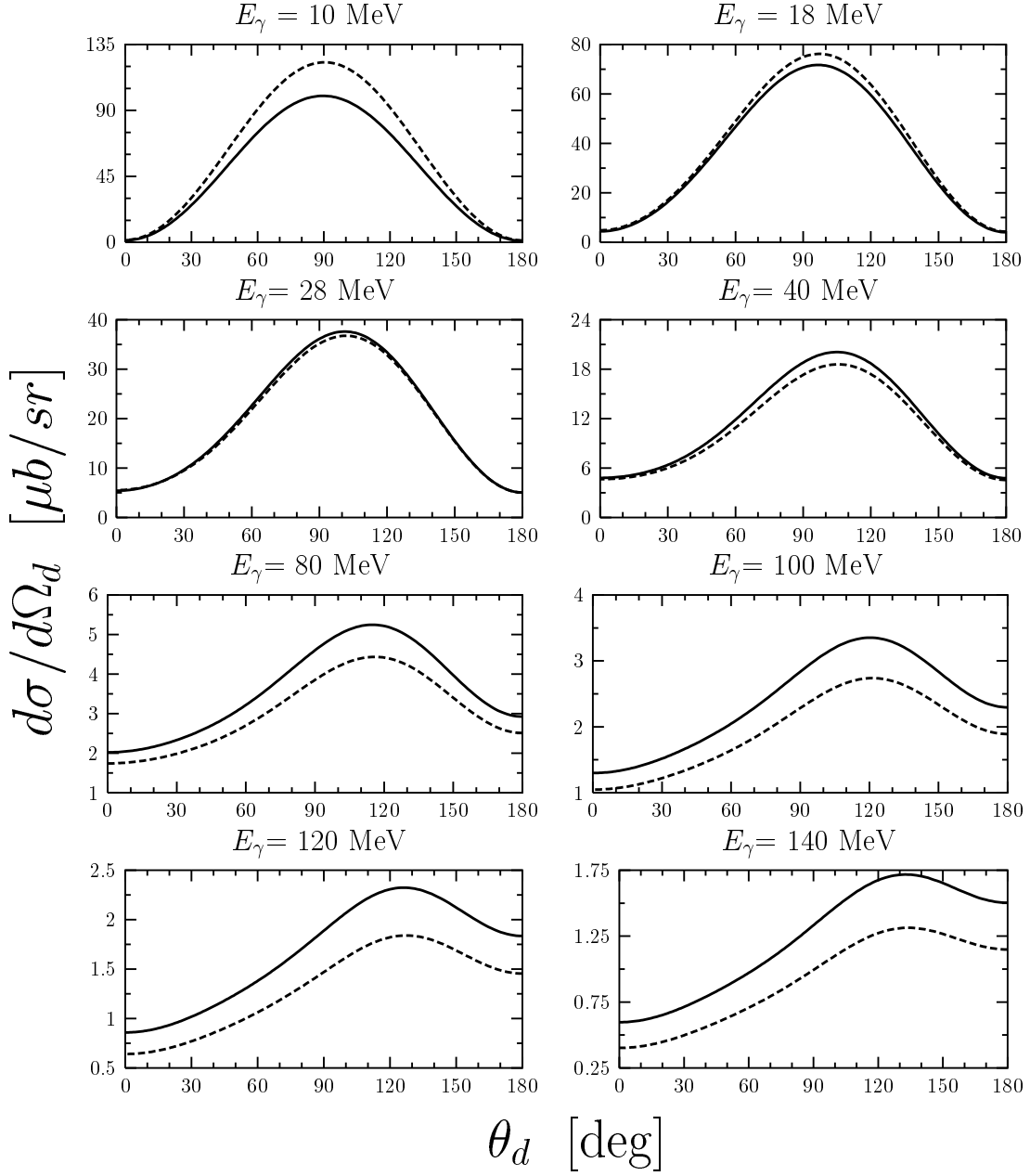


FIG. 1. Deuteron laboratory angular distribution for the process ${}^3\text{He}(\gamma, d)p$ at different photon energies E_γ . Curves show results of calculations with the AV18 NN and Urbana IX 3NF forces (solid) and with the AV18 NN force alone (dashed). The current is treated in the Siegert approach.

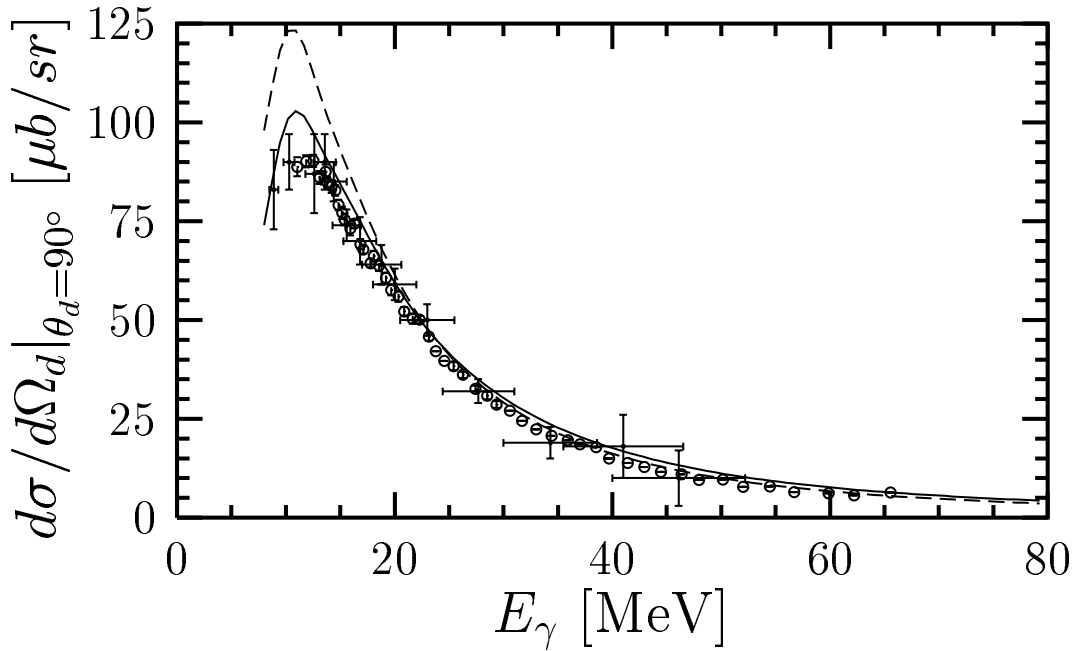


FIG. 2. Deuteron angular distribution for the process ${}^3\text{He}(\gamma, d)p$ at the given deuteron angle as a function of the photon energy E_γ . Curves as in Fig. 1. Since the kinematical shift from the laboratory to the c.m. system is not significant, we combine the data for the 90° laboratory angle (full dots with horizontal and vertical error bars [31]) with the ones for the 90° c.m. angle (open circles [30]).

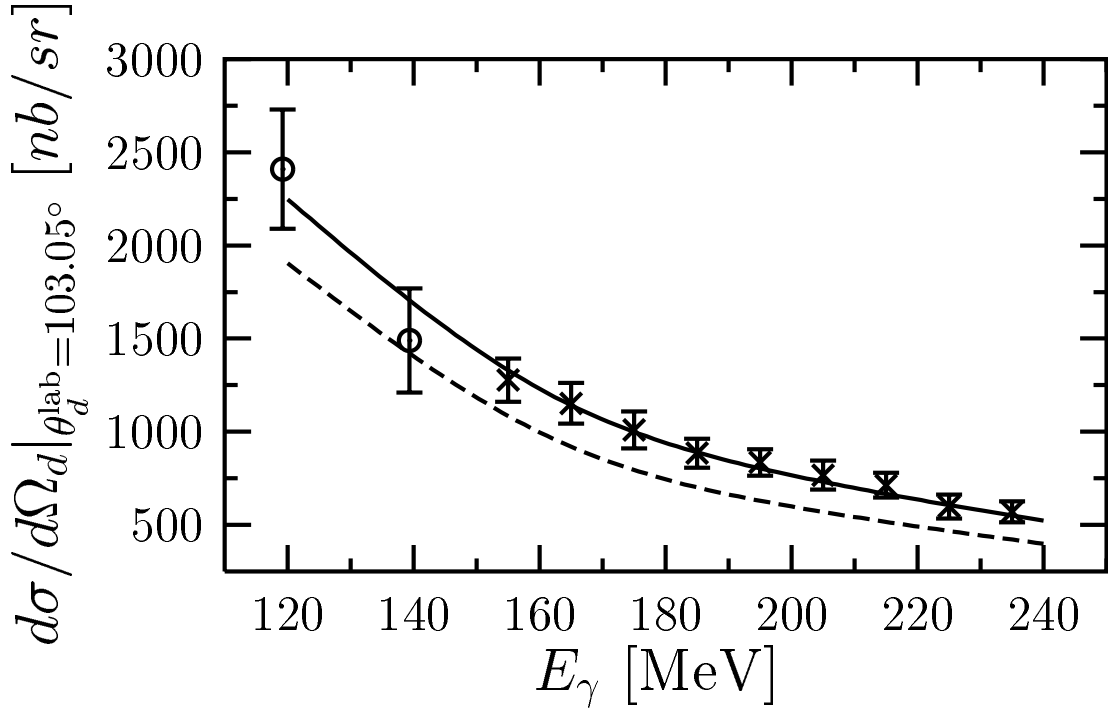


FIG. 3. Deuteron angular distribution for the process ${}^3\text{He}(\gamma, d)p$ at given laboratory angle as a function of the photon energy E_γ . Curves show results of calculations with the AV18 NN and Urbana IX 3NF forces (solid) and with the AV18 NN force alone (dashed). Explicit π - and ρ -like MEC's are included in the current operator. Data are from [32] (x-es) and [33] (circles).

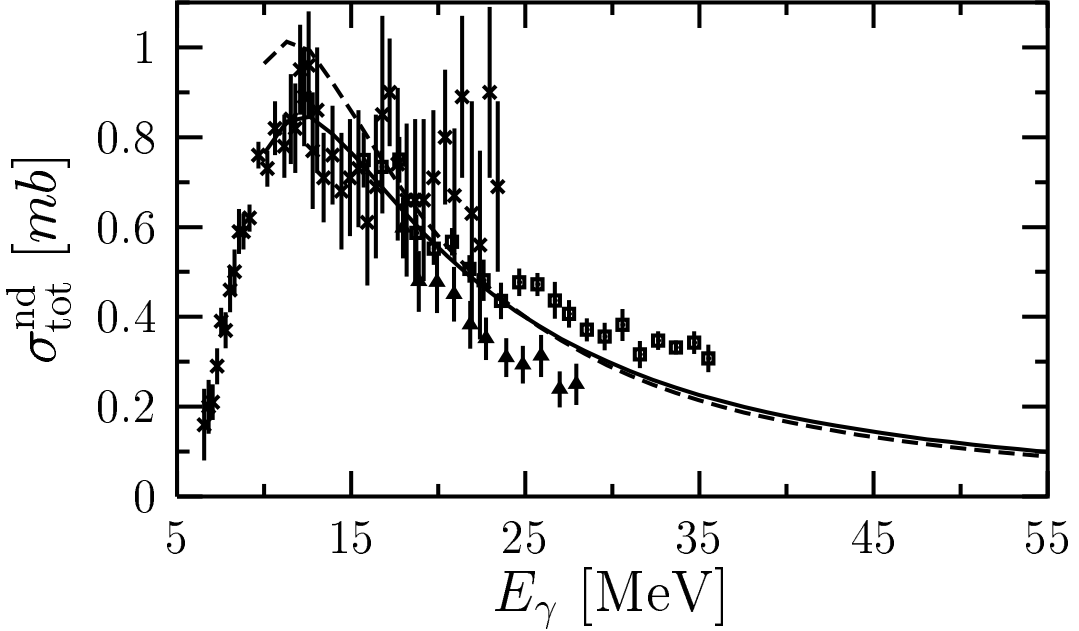


FIG. 4. Total cross section for the process ${}^3\text{H}(\gamma, d)n$ as a function of the photon laboratory energy E_γ . Curves as in Fig. 1. Data are from [34] (x-es), [35] (squares), [36] (triangles).

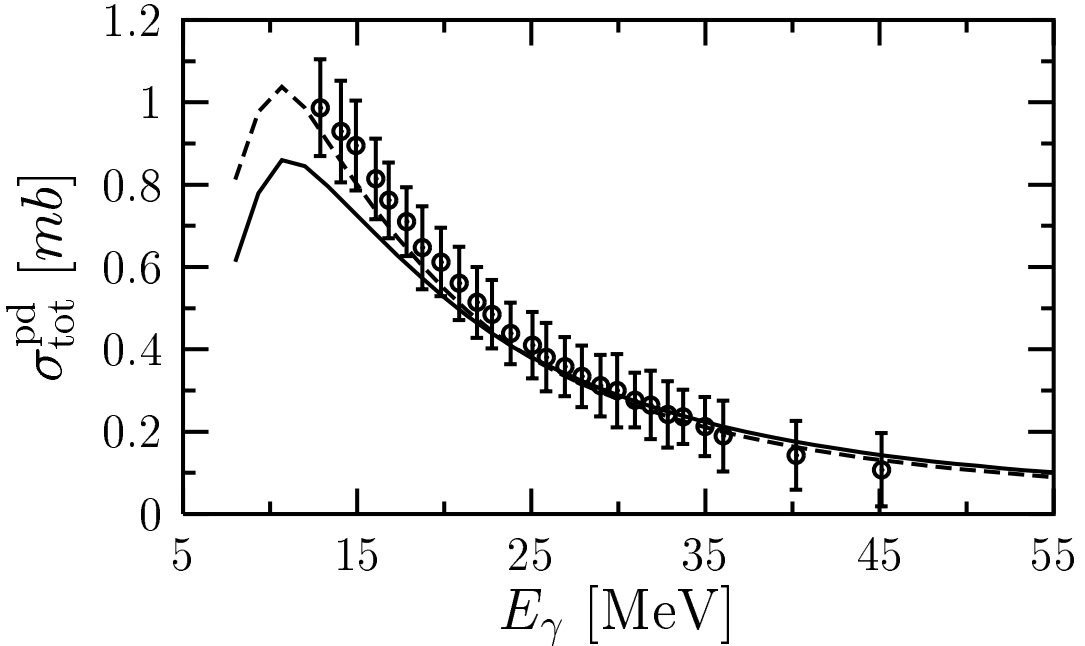


FIG. 5. Total cross sections for the ${}^3\text{He}(\gamma, d)p$ process as a function of the photon laboratory energy E_γ . Curves as in Fig. 1. Data are from [37].

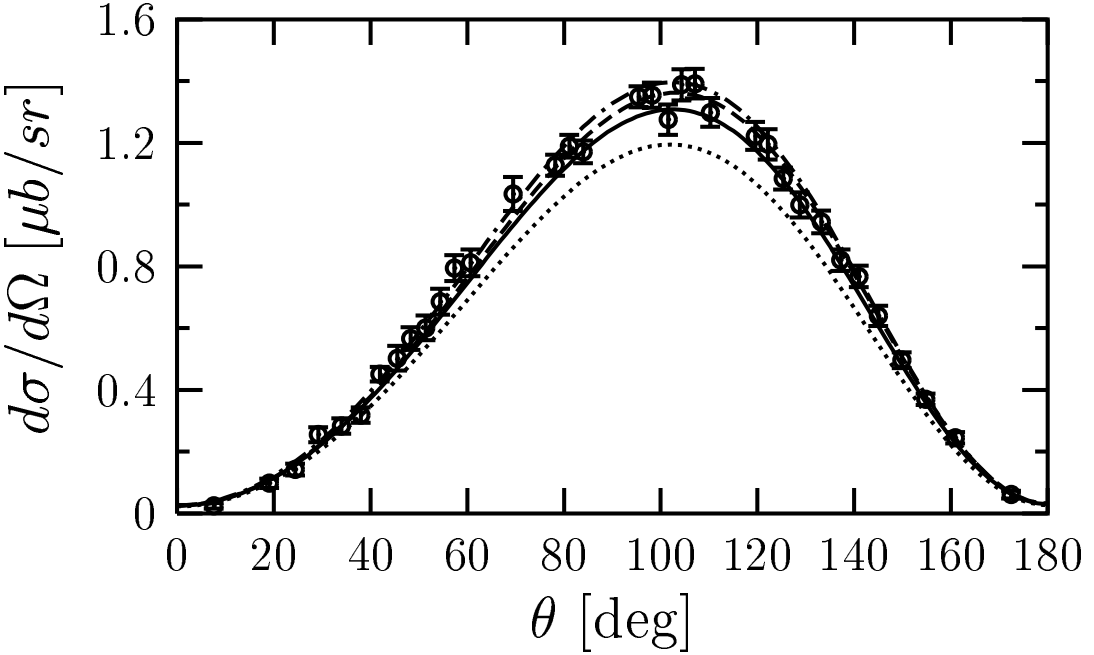


FIG. 6. The photon angular distribution for pd capture at $E_d = 19.8$ MeV against the c.m. γ -d scattering angle. The curves describe the Siegert (dashed-dotted), the single nucleon plus MEC (dashed), Siegert with 3NF (dotted) and the single nucleon plus MEC with 3NF (solid). These four cases are called a, b, a' and b' in the text. Data are from [38].

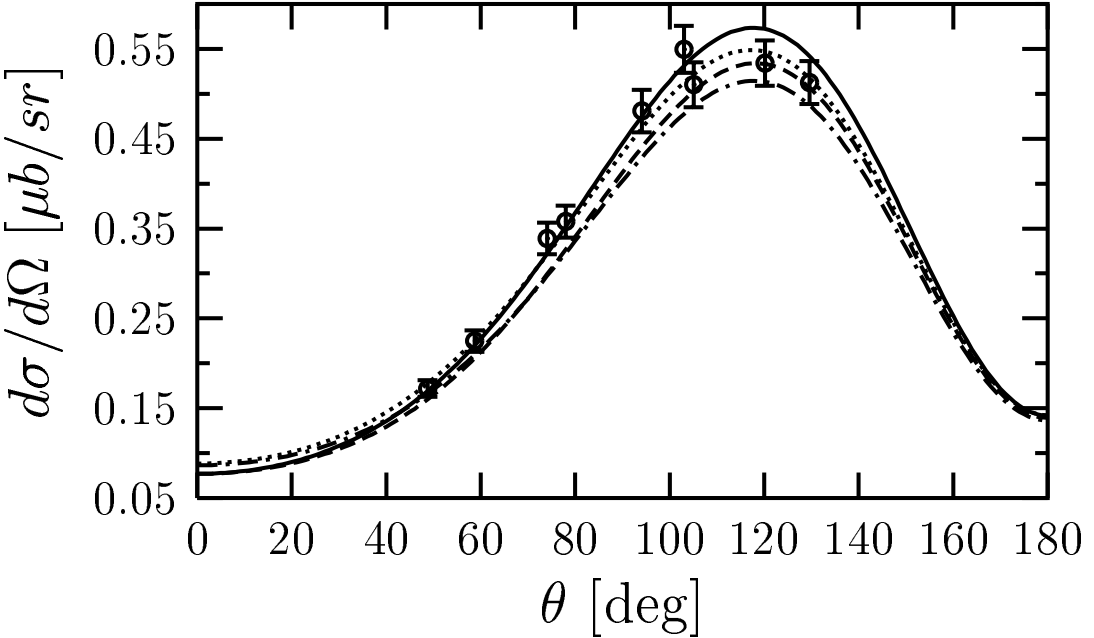


FIG. 7. The same as in Fig. 6 for $E_d = 95$ MeV. Data are from [39].

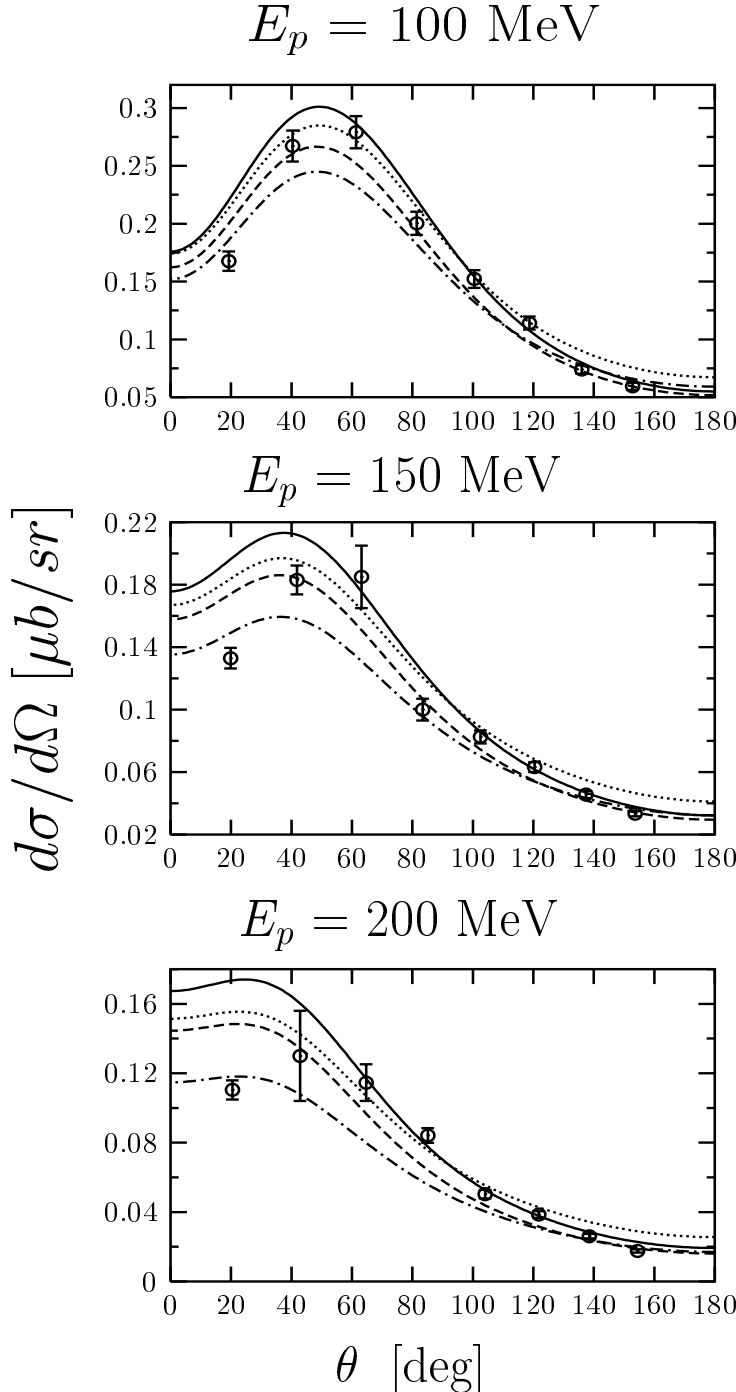


FIG. 8. The photon angular distribution for pd capture at three different proton laboratory energies against the c.m. γ -p scattering angle. Curves as in Fig. 6. Data are from [40].